Engineering Notes

ENGINEERING NOTES are short manuscripts describing new developments or important results of a preliminary nature. These Notes cannot exceed 6 manuscript pages and 3 figures; a page of text may be substituted for a figure and vice versa. After informal review by the editors, they may be published within a few months of the date of receipt. Style requirements are the same as for regular contributions (see inside back cover).

Static Measurements of Slender Delta Wing Rolling Moment Hysteresis

Joseph Katz*
San Diego State University, San Diego, California
and
Daniel Levin†
NASA Ames Research Center, Moffett Field, California

Introduction

MOST high-speed airplanes incorporate wings or strakes with considerable leading-edge aft sweep. Such wings, in addition to their favorable performance at supersonic speeds, are also capable of generating high lift coefficients for low-speed maneuvers and landing. The high lift at low speed is obtained by vortex lift, which is a result of concentrated vortices originating at the sharp leading edges of the lifting surfaces. However, flight tests[1] of such slender wings and wind tunnel tests[2–5] with free-to-roll delta wings indicate that this type of wing planforms is subject to self-induced roll oscillations. A typical experimental procedure to measure these roll oscillations (wing rock) is described schematically in Fig. 1. In this case,[3,4] a slender delta wing was set at an angle of attack α in the wind tunnel, and in most cases, the wind tunnel natural disturbance was sufficient to initiate a continuous limit cycle roll oscillation.

Analytical investigations[6–10] focused on aerodynamic hysteresis during the limit cycle roll oscillation as the cause of this phenomena. Among the reasons causing this nonlinearity (the hysteresis), time delays and asymmetry in the leading-edge vortex strength, motion, and vortex burst location were suggested. Experimental evidence, especially at low angles of attack[3] ($\alpha \approx 20$ deg), points toward momentary asymmetry in vortex strength and location as the driving moment for the oscillations. Calculated dynamic rolling moment hysteresis loops[2–4] (as shown in Fig. 1b) indicate that near the wing level condition (where the roll angle $\Phi \approx 0$) there is an undamped loop in the rolling moment data that is being balanced by the two damped loops at the two edges of the limit cycle (at large values of $|\Phi|$). This energy balance sustains the limit cycle roll oscillations.

It is believed that at the larger angles of attack the two outer damped loops are influenced by the vortex breakdown. This can be justified by considering the effect of roll rate on the downward rolling semispan of the wing that increases the local wing incidence, advances the leading-edge vortex burst on the corresponding wing side, reduces its lift, and, thereby, creates an incremental damping moment. Proof of this hypothesis, by direct measurement of the rolling moment during the unsteady oscillation, is rather complex and difficult, therefore, at this point, only the static rolling moment hysteresis (which is mainly a result of the vortex burst) is presented.

These data (in Figs. 2–5) were obtained by locking the free-to-roll axis bearings of the same experiment apparatus of

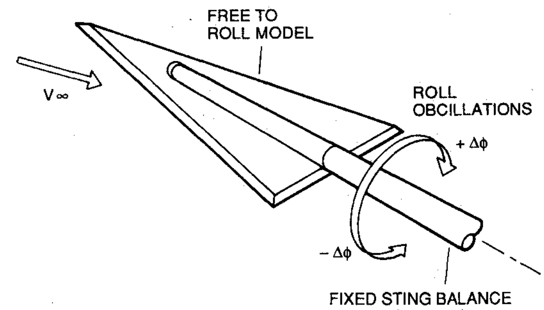

Fig. 1a Schematic description of the "wing-rock" experiment.

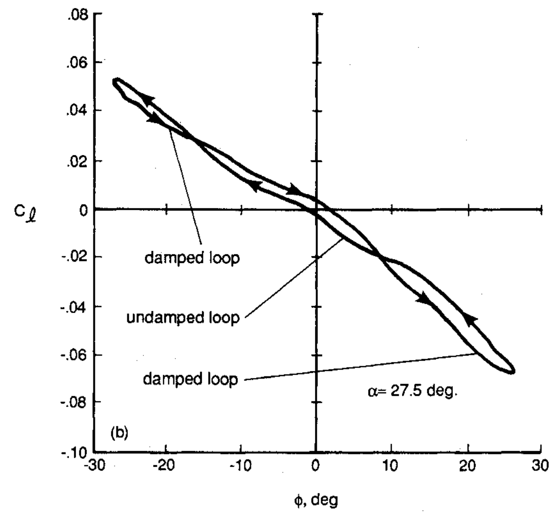

Fig. 1b Estimated rolling moment histogram during a limit cycle roll oscillation.

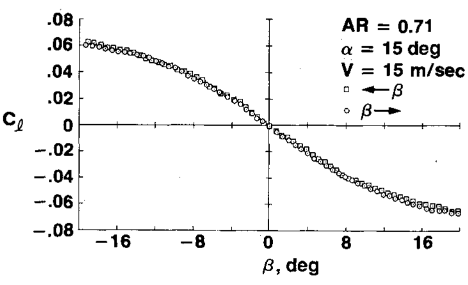

Fig. 2 Static rolling moment hysteresis during positive and negative side-slip sweeps ($\alpha = 15$ deg, $Re_c = 0.2 \times 10^6$).

Received May 6, 1989; revision received March 19, 1990.

*Professor, Department of Aerospace Engineering. Member AIAA.
†Senior NRC Research Associate. Member AIAA.

Ref. 3, which exhibited limit cycle roll oscillations. The static hysteresis data of Figs. 2–5, therefore, is different from the dynamic hysteresis since it does not have the central undamped driving loop (compared to Fig. 1b) and clearly cannot sustain limit cycle roll oscillations. Also, because of the steady-state nature of these experiments, these results should be viewed as an indication of the damping role of the vortex burst but not as a direct proof.

Discussion

The experimental apparatus that is shown schematically in Fig. 1 is the same hardware used for the dynamic load measurements during the roll oscillation tests reported in Refs. 3 and 4. The slender delta wing root chord was 428.5 mm, and span was 150 mm (aspect ratio = 0.71), and test Reynolds number, based on this root chord, was about $Re_c = 0.2 \times 10^6$. The wing leading edge was sharp and had a bevel of 30 deg, as shown in Fig. 1. This nonsymmetric leading-edge geometry has a noticable effect on the wing aerodynamics, and the difference in normal force due to inverting the wing is reported in Ref. 11. The wind tunnel was of an open return type, with a 1 × 1 m test section, and leading-edge vortex core positions were visualized by using the helium and soap bubble technique. The aerodynamic load measurements were conducted at a fixed angle of attack and then at very low rate (~0.5 rev/min). The side-slip angle β was varied by direct yaw motion of the string support. This experiment was mechanically much simpler than a roll angle variation experiment, but it still can provide valuable information about the rolling moment hysteresis. (Note the relation between side-slip and roll angles is $\tan\phi = \sin\beta/\sin\alpha$.)

The measured rolling moment for varying the side-slip angle between $\beta = \pm 20$ deg at an angle of attack of $\alpha = 15$ deg is shown in Fig. 2. At zero side slip, the leading-edge vortices are stable and no vortex burst is present over the wing. (Recall that flow visualization observations are based on the helium/soap bubble technique.) For the higher side-slip conditions ($\beta \approx |16| - |20|$ deg) there is a small indication of counterclockwise hysteresis. This becomes more evident in the case of $\alpha = 25$ deg in Fig. 3. Now if, for example, when increasing positive side slip (or equivalent positive roll angle) the restoring rolling moment is larger than in the decreasing side-slip situation, then work needs to be invested to sustain the equivalent rolling motion. Thus, a clockwise loop in the rolling moment data (or an undamped loop) will drive the motion, whereas a counterclockwise hysteresis (a damped loop—as here) will consume work or increase the damping of the system. This trend is repeated for the larger angles of attack in Figs. 4 and 5, but the large hysteresis loop occurs at smaller side-slip conditions because of the more advanced vortex burst position. The damping forces seem to be the largest in the case of $\alpha = 25$ deg, when the vortex burst is moving over the wing's trailing edge (at Fig. 3). In Fig. 4, the vortex burst, at $\beta = 0$, is near the trailing edge and any small value of side slip will move the vortex burst above the wing. (This will initiate the wing stall, as shown in Ref. 3.) For the $\alpha = 45$ deg case, the wing stall has been initiated and the vortex burst is ahead of the trailing edge at the $\beta = 0$ condition. Consequently, the hysteresis is smaller but maintains the damping characteristics (as shown by Fig. 5).

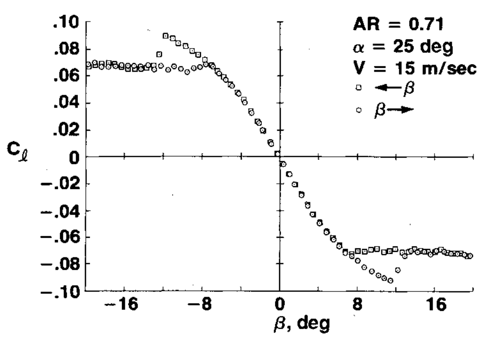

Fig. 3 Static rolling moment hysteresis during positive and negative side-slip sweeps ($\alpha = 25$ deg, $Re_c = 0.2 \times 10^6$).

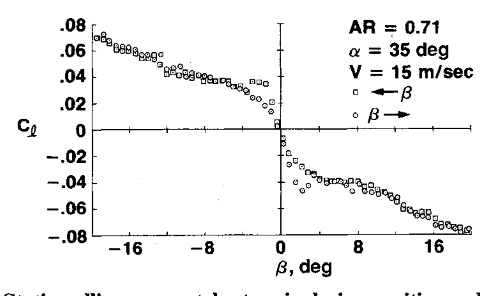

Fig. 4 Static rolling moment hysteresis during positive and negative side-slip sweeps ($\alpha = 35$ deg, $Re_c = 0.2 \times 10^6$).

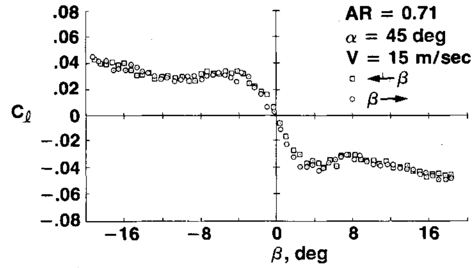

Fig. 5 Static rolling moment hysteresis during positive and negative side-slip sweeps ($\alpha = 45$ deg, $Re_c = 0.2 \times 10^6$).

Conclusion

The preceding tests clearly indicate that the static rolling moment hysteresis has a damping nature. This hysteresis seems to be larger when, due to wing roll (or side slip), the vortex burst moves back and forth over the wing trailing edge.

These static data should be viewed as an indirect indication of the damping role of the vortex burst during the limit cycle roll oscillations of slender delta wings, but not as a direct proof (and, therefore, further studies are needed).

Acknowledgments

This work was supported by NASA Ames Research Center, under Grant NCC-2-596, with James C. Ross as project monitor.

References

[1]Ross, A. J., "Investigation of Nonlinear Motion Experienced on a Slender-Wing Research Aircraft," *Journal of Aircraft*, Vol. 9, Sept. 1972, pp. 625–631.

[2]Nguyen, L. T., Yip, L., and Chambers, J. R., "Self Induced Wing Rock of Slender Delta Wings," AIAA Paper 81-1883, Aug. 1981.

[3]Levin, D., and Katz, J., "Dynamic Load Measurements with Delta Wings Undergoing Self-Induced Roll Oscillations," *Journal of Aircraft*, Vol. 21, Jan. 1984, pp. 30–36.

[4]Katz, J., and Levin, D., "Self-Induced Roll Oscillations Measured on a Delta Wing/Canard Configuration," *Journal of Aircraft*, Vol. 23, Nov. 1986, pp. 814–819.

[5]Jun, Y. W., and Nelson, R. C., "Leading Edge Vortex Dynamics on a Delta Wing Undergoing a Wing Rock Motion," AIAA Paper 87-0332, Jan. 1987.

[6]Schmidt, L. V., "Wing Rock Due to Aerodynamic Hysteresis," *Journal of Aircraft*, Vol. 16, March 1979, pp. 129–133.

[7]Konstadinopoulos, P., Mook, D. T., and Nayfeh, A. H., "Numerical Simulation of the Subsonic Wing Rock Phenomenon," AIAA Paper 83-2115, Aug. 1983.

[8]Ericsson, L. E., "The Fluid Mechanics of Slender Wing Rock," *Journal of Aircraft*, Vol. 21, May 1984, pp. 322–328.

[9]Ericsson, L. E., "Flow Phenomena Causing Wing and Body Rock," AIAA Paper 84-2177, Aug. 1984.

[10]Hsu, C. H., and Lan, C. E., "Theory of Wing Rock," *Journal of Aircraft*, Vol. 22, Oct. 1985, pp. 920–924.

[11]Katz, J., and Levin, D., "Measurement of Ground Effect for Delta Wings," *Journal of Aircraft*, June 1984, pp. 441–443.